nature structural & molecular biology

Retinal dynamics underlie its switch from inverse agonist to agonist during rhodopsin activation

Andrey V Struts[1,2], Gilmar F J Salgado[3], Karina Martínez-Mayorga[4] & Michael F Brown[1,5]

X-ray and magnetic resonance approaches, though central to studies of G protein–coupled receptor (GPCR)-mediated signaling, cannot address GPCR protein dynamics or plasticity. Here we show that solid-state ^{2}H NMR relaxation elucidates picosecond-to-nanosecond–timescale motions of the retinal ligand that influence larger-scale functional dynamics of rhodopsin in membranes. We propose a multiscale activation mechanism whereby retinal initiates collective helix fluctuations in the meta I–meta II equilibrium on the microsecond-to-millisecond timescale.

The molecular mechanisms of GPCR activation are the focus of considerable interest in cellular responses to biogenic amines and drugs, as well as in taste, olfaction, vision and a multitude of other biological signaling phenomena[1,2]. Knowledge of the three-dimensional structures of rhodopsin[3,4] and the β_2-adrenergic receptor[1] affords new opportunities for investigating GPCRs of human therapeutic significance. Despite the availability of crystal structures[1,4], understanding rhodopsin activation has been challenging because of the lack of atomic-level data for the signal-transducing meta II state of the protein[2]. We used solid-state ^{2}H NMR methods[5] to provide a new axis of information—the fourth dimension of time—needed to more fully interpret structural studies[4,6,7]. Our approach is quite different from previous ones, as we investigate the intrinsic mobility of the ligand that changes during visual light excitation.

To explore the energy landscape[8] for receptor activation, we measured ^{2}H NMR relaxation times[5] for the methyl (Me) groups[9] of retinal bound to rhodopsin in the dark, meta I and activated meta II states (**Supplementary Methods**). Knocking out any of the methyl groups yields back-shifting of the meta I–meta II equilibrium[9] and loss of function. An overview of rhodopsin light activation[10,11] illustrates the timescales of the major conformational transitions (**Fig. 1a**). Solid-state ^{2}H NMR spectroscopy of dark-state rhodopsin with retinal ^{2}H-labeled at the C5-, C9- or C13-Me groups yields similar residual quadrupolar couplings (**Fig. 1b**–**d**). Yet, pronounced variations are clearly evident in partially relaxed ^{2}H NMR spectra (**Fig. 1e**,**f**) and from inversion-recovery curves (**Fig. 1g**) used to determine spin-lattice (T_{1Z}) relaxation times.

A major strength of solid-state NMR spectroscopy is that membrane proteins are studied in a natural bilayer lipid environment[12]. Because the retinylidene methyl groups at the C5, C9 and C13 carbons (**Fig. 1**) strongly affect the meta I–meta II equilibrium[9], we conducted ^{2}H NMR relaxation measurements of these positions (**Supplementary Fig. 1**). Phosphoethanolamine head groups and unsaturated lipid acyl chains support rhodopsin activity[13]—that is, they shift the meta I–meta II equilibrium forward (whereas phosphocholine head groups shift it backward). Hence we used a 1-palmitoyl-2-oleoyl-*sn*-glycero-3-phosphocholine (POPC) bilayer to trap meta I, and a POPC bilayer containing 1,2-dioleoyl-*sn*-glycero-3-phosphoethanolamine (DOPE) to trap meta II, as shown by UV-visible spectrophotometry (**Supplementary Fig. 2**). These results are explained by matching of the spontaneous (intrinsic) monolayer curvature (H_0) to the membrane bilayer; POPC, with $H_0 \approx 0$, favors meta I, whereas DOPE has $H_0 < 0$ and favors meta II[13]. Such concepts of lipid-protein interactions have been previously reviewed[13] and are receiving increased attention.

In the dark state, deformation of retinal[12,14–16] (induced fit) produces striking differences in methyl dynamics that are clearly evident in the ^{2}H T_{1Z} relaxation times (**Fig. 2**). Arrhenius-type plots of the T_{1Z} data against inverse temperature for the retinylidene ligand in the dark, meta I and meta II states are indeed unexpected: the T_{1Z} times for the C9- and C13-Me groups increase with temperature, whereas those for C5-Me show a distinct minimum (**Fig. 2a**). Briefly, the T_{1Z} minimum occurs at higher temperature (to the left) for slower motions (smaller pre-exponential factor and/or larger activation energy, E_a) and, conversely, at lower temperature (to the right) for faster motions (larger pre-exponential factor and/or smaller E_a). At the T_{1Z} minimum, effective correlation times (τ_c) for methyl spinning are related to the nuclear Larmor (resonance) frequency (ω_0) by $\tau_c \approx 1/\omega_0$ because of matching of the power spectrum of the fluctuations to the nuclear spin energy gap. For the C5-Me group, the correlation time for the motions is $\tau_c > 13$ ns below −100 °C. Notably, for the C9- and C13-Me groups, the minimum falls outside the observed range (<−160 °C), so that $\tau_c < 1/\omega_0 \approx 13$ ns (see below).

The light-induced changes in the retinylidene dynamics are encapsulated by pronounced T_{1Z} differences in the meta I and meta II states (**Fig. 2b**,**c**). The short T_{1Z} relaxation times of the C5-Me group suggest the β-ionone ring maintains a predominantly 6-*s*-*cis* conformation[12], rather than a 6-*s*-*trans* conformation as in bacteriorhodopsin[17]. Notably[18], the β-ionone ring is little affected by transitions among the dark, meta I and meta II states—it retains nearly the same

[1]Department of Chemistry, University of Arizona, Tucson, Arizona, USA. [2]Department of Physics, St. Petersburg State University, St. Petersburg, Russia. [3]Département de Chimie, École Normale Supérieure, Paris, France. [4]Torrey Pines Institute for Molecular Studies, Fort Pierce, Florida, USA. [5]Department of Physics, University of Arizona, Tucson, Arizona, USA. Correspondence should be addressed to M.F.B. (mfbrown@u.arizona.edu).

Received 9 June 2010; accepted 16 November 2010; published online 30 January 2011; doi:10.1038/nsmb.1982

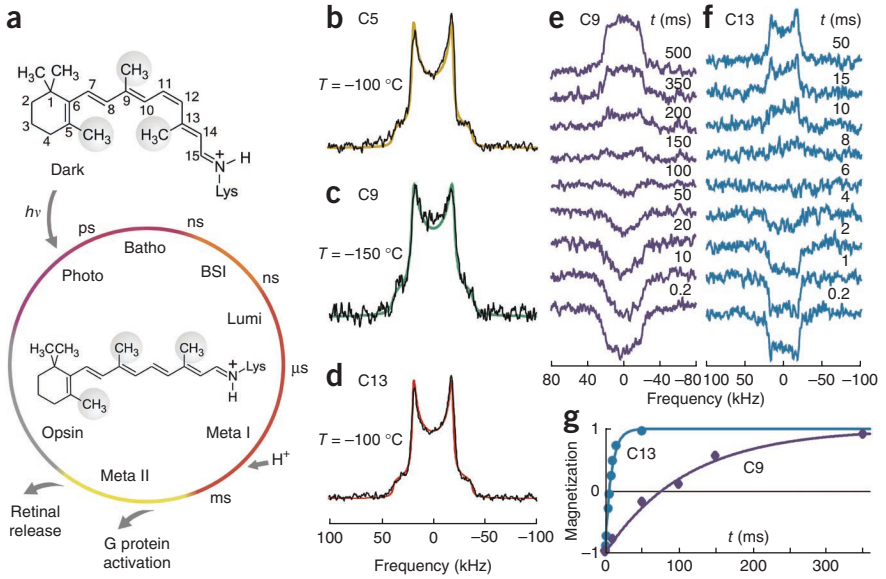

Figure 1 Site-specific ^{2}H NMR relaxation illuminates functional dynamics of retinylidene methyl groups within binding pocket of rhodopsin. (**a**) Light absorption yields *cis*-to-*trans* isomerization at position 11, converting retinal from an inverse agonist to an agonist through series of rhodopsin intermediates (designated photo, batho, blue-shifted intermediate (BSI), lumi, meta I, meta II) with different time scales. (**b**–**d**) Solid-state ^{2}H NMR spectra for dark-state rhodopsin with 11-*cis*-retinal deuterated at C5, C9 or C13 with C^{2}H$_3$ groups in POPC bilayers (1:50 molar ratio). The ^{2}H NMR line shapes indicate rapid axial spinning of C–C^{2}H$_3$ groups down to at least –160 °C. (**e**,**f**) Partially relaxed ^{2}H NMR spectra for retinylidene C9- and C13-Me groups of rhodopsin in aligned POPC membranes ($\theta = 0°$) at –150 °C. (**g**) Inversion-recovery plots showing site-specific variations in spin-lattice (T_{1Z}) relaxation times for C9- and C13-Me groups at –150 °C.

local environment[12]. A shift of the T_{1Z} minimum for the C5-Me to lower temperatures in meta II (**Fig. 2c**) implies a decrease in the local correlation time that may, for example, be due to lowering of E_a caused by a change in the C6–C7 torsional angle and/or increased ring mobility. For the functionally critical[9] C9-Me group, a marked shift in T_{1Z} is seen in meta I and meta II that manifests as an increase in E_a for methyl spinning within the binding pocket of rhodopsin. The similar E_a barriers of the C9- and C13-Me groups observed after 11-*cis*–to–all-*trans* isomerization are logical, as the two groups are now on the same side of retinal (**Fig. 2b**,**c**).

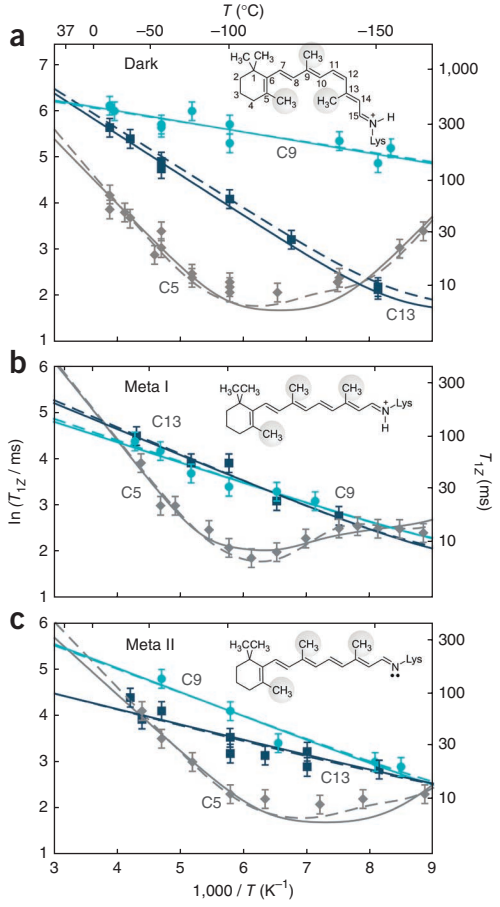

Next, we applied NMR relaxation theory[5] to analyze the molecular dynamics of retinal bound to rhodopsin. The T_{1Z} times were analyzed using either a three-site jump model or a continuous diffusion model for rotation of the retinylidene methyl groups[5]. Although the order parameters have little variation, large site-specific differences are evident in the pre-exponential factors and activation barriers (E_a) (**Fig. 3a**). For the C5-Me of the β-ionone ring (E_a = 10–15 kJ mol^{-1}), the values exceed those of the other methyl groups in the dark, meta I and meta II states. Unexpectedly, the C5-Me barrier stays nearly unaltered up to meta II, consistent with a predominantly 6-*s*-*cis* conformation of the β-ionone ring[12]. Perhaps most strikingly, however, the C9-Me group—which is essential to rhodopsin function[9]—is literally a dynamic hot spot. Based on our quantum mechanical calculations (not shown), the remarkably small barrier to rotation of the C9-Me group (E_a = 2 kJ mol^{-1} in the dark state) (**Fig. 3a**) arises from nonbonded (1,6) interactions with hydrogen atoms H7 and H11 of the polyene chain (see **Fig. 1a**). By contrast, for the C13-Me group near the protonated Schiff base (PSB), the barrier is greater, owing to nonbonded (1,7) interactions with hydrogen H10. Upon 11-*cis*–to–*trans* isomerization (**Fig. 1a**), (1,6) interactions of the C13-Me group occur with both polyene hydrogens H11 and H15, so the C13-Me barrier (E_a = 3–5 kJ mol^{-1}) becomes comparable to the C9-Me barrier in the meta I and meta II states. Notably, in the sequence dark–meta I–meta II, there is a progressive increase in E_a for the C9-Me of the polyene chain, accompanied by a decrease for the C13-Me (**Fig. 3a**).

Rhodopsin (1U19)[3] with retinal[12] inserted into the ligand-binding cavity allows us to propose how local picosecond- to nanosecond-scale motions detected by ^{2}H NMR correspond to large-scale microsecond-scale functional protein motions (**Fig. 3b**,**c**)[6,10]. In the dark state, the low activation barrier of the C9-Me group signifies the absence of

Figure 2 Solid-state ^{2}H NMR captures site-specific changes in retinal mobility during light activation of rhodopsin. (**a**–**c**) Spin-lattice (T_{1Z}) relaxation times (±s.d.) of retinylidene methyl groups are shown versus reciprocal temperature in the dark (**a**), meta I (**b**) and meta II (**c**) states (–30 to –160 °C). Methyl dynamics are described by an axial three-fold jump model or a continuous diffusion model with coefficients $D_{||}$ and $D_{\perp}$. In **a**–**c**, rotation about the methyl threefold (C_3) axis corresponds to solid lines with $D_{\perp} = 0$; the dashed lines include restricted off-axial diffusion ($D_{\perp} = D_{||}$). Fits for the C5-Me in meta I in **b** assume unlike rotational diffusion constants ($D_{||} \neq D_{\perp}$) (dashed line) or the presence of two conformers with different bond orientations and axial diffusion coefficients (solid line).

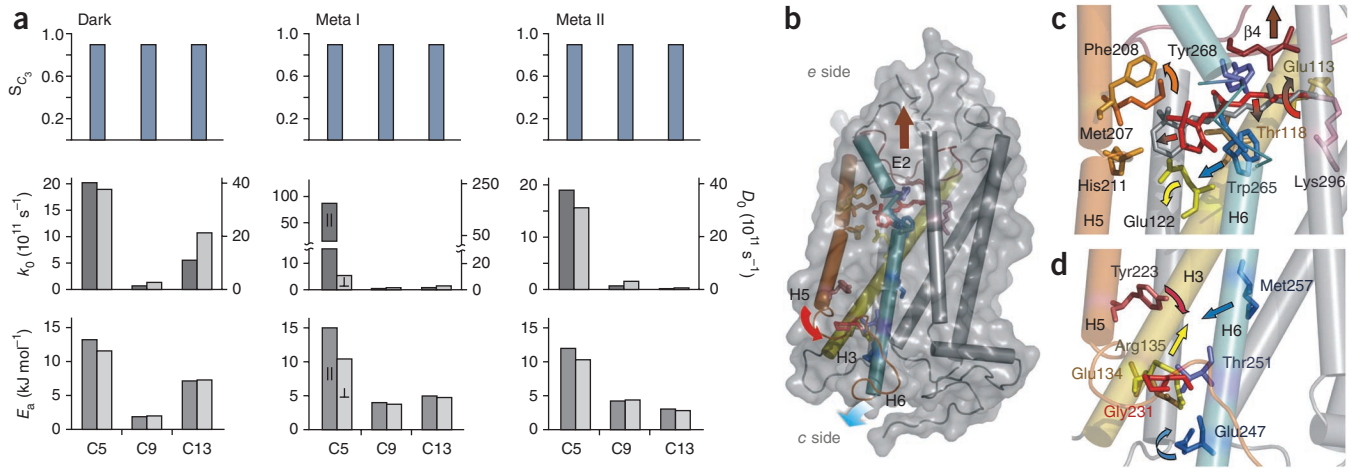

Figure 3 ^{2}H NMR relaxation of retinal sheds new light on activation mechanism of rhodopsin. (**a**) Summary of analysis of solid-state ^{2}H NMR measurements. Order parameters of rapidly spinning methyl groups are designated by S_{C_3}; the pre-exponential factor is k_0 for three-fold axial jumps or D_0 for continuous diffusion; and E_a indicates the activation energy. (The diffusion model assumes either $D_\perp = 0$ (right) or $\eta_D \equiv D_\parallel/D_\perp = 1$ (left) except for the C5-Me in meta I, where $\eta_D \neq 1$.) (**b**–**d**) Proposed activation mechanism for rhodopsin in membranes based on X-ray[19], FTIR[11] and ^{2}H NMR data[12]. Isomerization of retinal displaces the E2 loop toward the extracellular (*e*) side, with fluctuations of helices H5 and H6 exposing transducin (G_t) recognition sites on the opposing cytoplasmic (*c*) surface. Figure produced (PDB 1U19)[3] using PyMOL (http://pymol.sourceforge.net/).

steric clashes, as it occupies a slot between Tyr268 and Thr118. In the meta I NMR structure of retinal[12], the C9-Me acts effectively as a hinge point for retinal isomerization, causing the C13-Me and the C = NH^+– groups to change orientation. Rotation of the C13-Me displaces the β_4 strand of the E2 loop toward the extracellular (*e*) side (**Fig. 3c**), disrupting a hydrogen bonding network involving transmembrane helices H4–H6, as suggested by a decrease in E_a for the C13-Me group. At the opposite end of retinal, the β-ionone ring is displaced toward the H3–H5 helical interface, giving a tighter packing for the C5-Me indicated by the relatively high E_a value in the meta I state (**Fig. 3a**). The ionic lock involving the retinylidene PSB on H7 with its complex counterion due to Glu113 (H3) and Glu181 (E2) is broken by internal proton transfer from the PSB to Glu113 in meta II. Straightening of retinal causes the β-ionone ring to move away from Trp265 (H6) toward Glu122 (H3), disrupting a second hydrogen bonding network connecting transmembrane helices H3 and H5 (ref. 12). Initial movement of helix H6 from the H1–H4 helical core is accompanied by displacement of helix H5, bringing Tyr223 closer to Arg135 and Gly231 near to Glu247 (**Fig. 3d**)[19]. Destabilization of the charge adduct of Glu134 and Arg135 of the Glu(Asp)-Arg-Tyr (E(D)RY) sequence of helix H3 with Glu247 of helix H6[19] yields transient exposure of transducin (G_t) recognition elements on the cytoplasmic (*c*) side (**Fig. 3b**). Receptor activation is further driven by protonation of Glu134 from the aqueous medium[11].

According to the above picture, rhodopsin activation involves collective fluctuations of transmembrane helices H5 and H6 and the cytoplasmic loops in the meta I–meta II equilibrium. The reversible helix movements[10,11] occur at kilohertz frequencies and match the catalytic turnover rate for G_t binding and activation by rhodopsin[20]. Receptor activation is due to a fluctuating equilibrium among states and substates[10,11]—an arresting illustration of the role of conformational entropy in GPCR biology. A key unanswered question is whether it will eventually be possible to quantitatively trap a unique activated rhodopsin conformation, or whether the receptor function is inextricably linked to dynamics of a conformational ensemble unlocked by photoisomerization of the retinal ligand.

Note: Supplementary information is available on the Nature Structural & Molecular Biology website.

ACKNOWLEDGMENTS

We thank T.A. Cross, K.P. Hofmann, M. Hong, W.L. Hubbell, L.E. Kay, S.O. Smith and R.W. Pastor for discussions. Retinal was provided by K. Tanaka, S. Krane and K. Nakanishi (Columbia University). Financial support from the US National Institutes of Health (EY012049 and EY018891) is gratefully acknowledged.

AUTHOR CONTRIBUTIONS

A.V.S. and M.F.B. designed the research. A.V.S. and G.F.J.S. performed the experiments. A.V.S., G.F.J.S., and K.M.-M. analyzed the data. A.V.S. and M.F.B. wrote the paper.

COMPETING FINANCIAL INTERESTS

The authors declare no competing financial interests.

Published online at http://www.nature.com/nsmb/.
Reprints and permissions information is available online at http://npg.nature.com/reprintsandpermissions/.

1. Kobilka, B. & Schertler, G.F.X. *Trends Pharmacol. Sci.* **29**, 79–83 (2008).
2. Ahuja, S. & Smith, S.O. *Trends Pharmacol. Sci.* **30**, 494–502 (2009).
3. Okada, T. *et al. J. Mol. Biol.* **342**, 571–583 (2004).
4. Ridge, K.D. & Palczewski, K. *J. Biol. Chem.* **282**, 9297–9301 (2007).
5. Brown, M.F. *J. Chem. Phys.* **77**, 1576–1599 (1982).
6. Altenbach, C., Kusnetzow, A.K., Ernst, O.P., Hofmann, K.P. & Hubbell, W.L. *Proc. Natl. Acad. Sci. USA* **105**, 7439–7444 (2008).
7. Ahuja, S. *et al. J. Biol. Chem.* **284**, 10190–10201 (2009).
8. Frauenfelder, H. *et al. Proc. Natl. Acad. Sci. USA* **106**, 5129–5134 (2009).
9. Vogel, R. *et al. Biochemistry* **45**, 1640–1652 (2006).
10. Knierim, B., Hofmann, K.P., Ernst, O.P. & Hubbell, W.L. *Proc. Natl. Acad. Sci. USA* **104**, 20290–20295 (2007).
11. Mahalingam, M., Martínez-Mayorga, K., Brown, M.F. & Vogel, R. *Proc. Natl. Acad. Sci. USA* **105**, 17795–17800 (2008).
12. Struts, A.V. *et al. J. Mol. Biol.* **372**, 50–66 (2007).
13. Brown, M.F. *Chem. Phys. Lipids* **73**, 159–180 (1994).
14. Verdegem, P.J.E., Bovee-Geurts, P.H.M., de Grip, W.J., Lugtenburg, J. & de Groot, H.J.M. *Biochemistry* **38**, 11316–11324 (1999).
15. Spooner, P.J.R. *et al. Biochemistry* **42**, 13371–13378 (2003).
16. Kukura, P., McCamant, D.W., Yoon, S., Wandschneider, D.B. & Mathies, R.A. *Science* **310**, 1006–1009 (2005).
17. Copié, V. *et al. Biochemistry* **33**, 3280–3286 (1994).
18. Borhan, B., Souto, M.L., Imai, H., Shichida, Y. & Nakanishi, K. *Science* **288**, 2209–2212 (2000).
19. Park, J.H., Scheerer, P., Hofmann, K.P., Choe, H.-W. & Ernst, O.P. *Nature* **454**, 183–188 (2008).
20. Ernst, O.P., Gramse, V., Kolbe, M., Hofmann, K.P. & Heck, M. *Proc. Natl. Acad. Sci. USA* **104**, 10859–10864 (2007).